Review Article

Cardiovascular Medicine in SPring-8

Cardiovascular diseases are the number one cause of death globally. To elucidate the underlying mechanisms of cardiovascular diseases, it is necessary to advance our understanding of structural and functional properties of the heart and vascular system under normal conditions as well as the dynamic changes under pathological conditions. SPring-8 provides several advanced experimental techniques for studying cardiovascular structure and function. This review focuses on three novel techniques: microangiography, X-ray diffraction, and high-resolution phase contrast tomography.

Microangiography

The resistance vessels of the microcirculation (~30-200 μm diameter, arterioles-small arteries) are the target points of various cardiovascular diseases. The vascular tone of these vessels is meticulously modulated via multiple mechanistic pathways including the vascular endothelium and smooth muscle as well as neurohumoral stimuli to control the resistance to the flow and hence optimize blood flow at the local tissue and whole-organ levels. Impairment of any of these regulatory systems adversely affects the vascular control of blood flow with abnormal vascular constriction and remodeling and, thus, increases the likelihood of lethal events such as myocardial infarction, stroke and hypertension. For a better understanding of the control of blood flow, it is necessary to directly measure the internal diameter (ID) and flow velocity in resistance vessels.

X-ray contrast absorption imaging techniques, such as cineangiography, have the advantage that X-rays pass through tissues more easily than light without exposing the organ of interest, making it possible to obtain a dynamic overview of the entire vascular network deep within an intact organ in real-time. Using conventional X-ray tubes, it is not currently possible to obtain images with exposure times of less than 10 ms and a spatial resolution better than 100 μm [1]. Synchrotron radiation (SR) absorption microangiography has been developed for the high-spatial resolution (up to 4.5 μm resolution) and high-speed (few milliseconds) imaging of resistance vessels by improving the single-energy temporal subtraction technique at beamline BL28B2 in SPring-8 [1]. SR has several distinct superior qualities compared with conventional angiography. In essence, SR is characterized by high brilliance and extreme collimation (minimal divergence of X-ray photons), allowing greater image contrast and sharpness without magnification artifacts for vessels at different depths. The high X-ray intensity also allows a greater flux even during a short exposure time to produce blur-free images of the hearts of small animals with a high heart rate (>500 beats/min). Rapid imaging (1-2 ms shutter open times) permits the accurate analysis of vessel diameters in a beating heart based on individual image frames without artifacts due to organ motion. SR allows selective tuning of the X-ray energy (33.2 keV, slightly higher than the iodine *K*-edge energy) with a monochromator, maximizing the difference in photon absorption between an iodine contrast agent in the vessels and surrounding tissues.

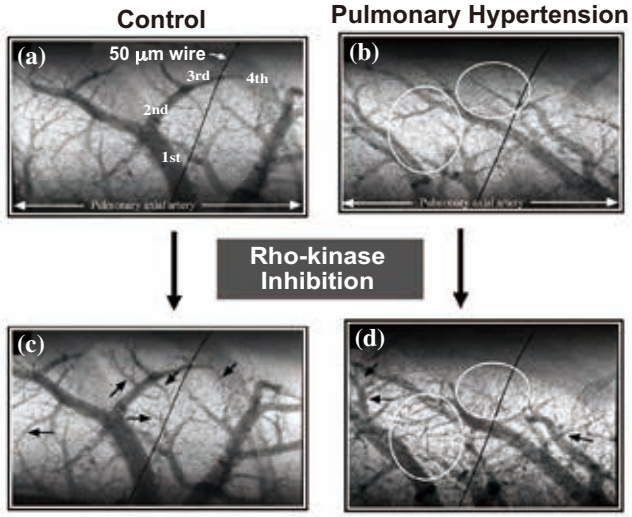

Fig. 1. Representative microangiograms showing the branching pattern of rat pulmonary arteries in control **(a, c)** and pulmonary hypertension **(b, d)** before **(a, b)** and following **(c, d)** Rho-kinase inhibiton. The black arrows indicate pulmonary arteries that have dilated as a result of Rho-kinase inhibition. The open white circles in image **(b)** indicate regions with few opaque vessels, which subsequently, in image **(d)**, appear to increase in vessel density following Rho-kinase inhibition, due to the reperfusion of previously constricted vessels. This was evident only in hypertensive rats.

SR microangiography has now been used for repeated visualization of the microcirculation in various organs such as the heart, lungs, brain, kidneys and hind limbs, especially in small animals [1,2]. SR allows us to identify resistance vessels with localized or nonuniform constriction and to characterize the extent of dysfunction of the vascular endothelium and smooth muscle in disease states. One prominent example is microangiography experimentation on rat models of pulmonary arterial hypertension [1,3,4], which is an intractable disease attracting much attention. The activation of Rho-kinase is increasingly recognized to be involved in the pathogenesis of this lethal disease. Recently, microangiography has revealed that the inhibition of Rho-kinase causes the dramatic emergence of pulmonary arterioles (< 100 μm ID) that were not visibly opaque in monocrotaline-induced rat pulmonary hypertension (Fig. 1) [3]. This appearance of "new" vessels indicates that severe Rho-kinase-mediated vasoconstriction restricts the pulmonary blood flow distribution by occluding the arterioles, which contravenes the long-held paradigm that pulmonary vessel rarefaction was the sole cause of vessel density reduction in pulmonary hypertension. It is very difficult to detect such regional microvascular dysfunction by using any other intravital methods including microscopy, CT and MRI.

High-resolution, high-speed angiography permits studies on a living mouse, and the coronary and pulmonary arterioles (~50 μm < ID) have been successfully visualized (Fig. 2) [1,5], allowing the analysis of genetic and molecular mechanisms for cardiovascular and pulmonary diseases at the whole-body level by using specific gene-targeted knockout and knockin mice. When vessel diameters are <50 μm ID and sequential images are not confounded by vessel movement, such as in the brain, image summation is also used to enhance the vessel morphology. SR microangiography has shed new light on the control of blood pressure and flow in health and disease.

X-Ray Diffraction of Cardiac Muscle

Many techniques are used to investigate how cardiac performance is regulated at the sarcomeric level in the heart. However, none of these techniques directly examines the movement or activity of the contractile proteins in the beating heart. The most significant advantages of X-rays are its high penetration power, which is used in medical diagnosis, and its short wavelength, which enables us to investigate structures at the atomic level. Combining these advantages enable us to investigate interactions between contractile proteins in muscle cells [6].

There is a hexagonal lattice of contractile filaments in muscle cells (Fig. 3(a)). The regular arrangement with a spacing of 30-40 nm gives rise to X-ray diffraction spots called equatorial reflections (Fig. 3(b)). The position of the spots represents the distance between filaments, while their intensity is related to the location of myosin heads that span filaments to produce the contractile force. The measurement of these reflections provides information on the molecular events taking place in cardiac cells. To examine a beating whole heart, an X-ray with a high energy (15 keV) that has high penetration power is necessary. By exposing a whole heart to a finely collimated intense beam at BL40XU (dimensions, 0.2×0.2 mm^2) it is possible to record the diffraction peaks in a myocardial region without averaging over multiple heart beats. Although there are layers of muscle fibers running in different directions in the heart wall, it is possible to account for the diffraction pattern recorded at different angles and depths in the heart [7].

Open-chest heart preparation allows a researcher to investigate regional differences in cross-bridge dynamics because the myocardial regions exposed to the beam can be determined [8]. Ventricular pressure and volume can be measured simultaneously. Figures 3(c) and 3(d) show the intensity changes of the equatorial reflections together with left ventricular (LV) pressure-volume recordings of the heart. Figure 3(c) was obtained from a normal rat heart while Fig. 3(d) was recorded in the same region of the heart after 30 min of ischemia (caused by occlusion of the coronary artery) followed by the reperfusion of blood. The figures show how the myosin mass transfer (cyclic changes in intensity ratio) can be estimated from continuous short SAXS recordings and how this localized index is altered by an episode of ischemia-reperfusion, whereas the ventricular pressure remains preserved in the same heart.

Recently, using this X-ray diffraction technique on a rat, it was demonstrated that contractile proteins in cardiac muscle cells that were derived from iPS cells and transplanted to an infarcted heart regularly operate in synchrony with the host heart (Fig. 4) [9].

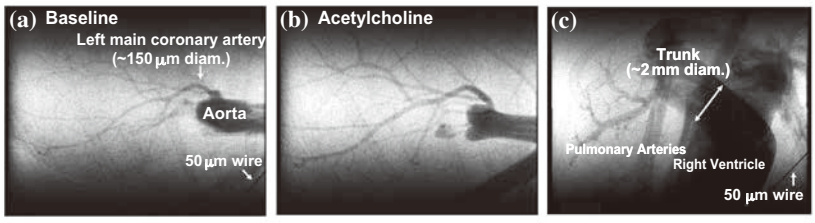

Fig. 2. Coronary and cardiopulmonary microangiograms of the intact chest in a living mouse. The small size of the mouse heart permits coronary imaging of the whole heart **(a)** and evaluation of endothelial stimulation (acetylcholine 5 μg/kg/min, **b**). Fast image acquisition of the mouse lungs enables visualization of multiple branching orders of pulmonary arteries and estimation of pulmonary blood flow transit time **(c)**.

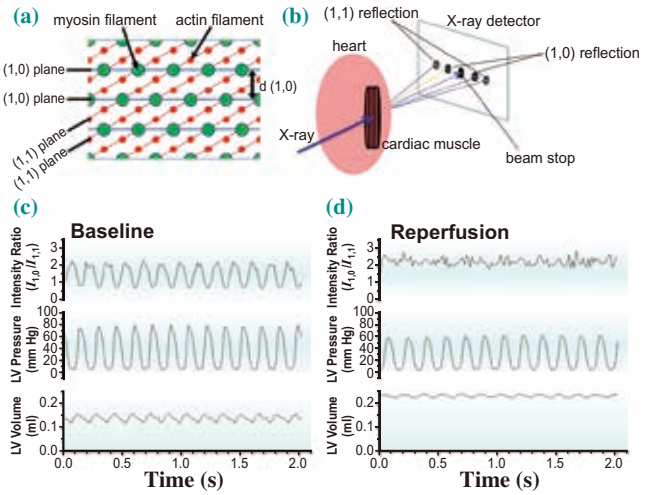

Fig. 3. X-ray diffraction from cardiac muscle. **(a)** Cross-section of the hexagonal lattice of myosin filaments (green) and actin filaments (red). In cardiac muscle, four diffraction peaks appear symmetrically at right angles to the filament lattice: the (1,0) and (1,1) reflections. **(c)** and **(d)**, Time traces of intensity ratio ($I_{1,0}/I_{1,1}$), left ventricular pressure and volume.

Cardiac muscle regeneration with iPS cells is regarded as the next-generation cardiac therapy. This work provided important evidence for the development of next-generation therapy for cardiac diseases by combining two leading-edge technologies, iPS cells and SPring-8, which originated in Japan.

Phase-contrast Microtomography

Radiographs are formed by the attenuation of X-rays by an object. It has been pointed out that the phase shift of an X-ray by an object is much larger than its attenuation, and thus, phase-contrast imaging is more sensitive (up to 1000 times) to small density differences than absorption-contrast imaging [10]. To measure phase shifts for imaging, an optical device called an interferometer is required. A grating-based interferometer ("Talbot" type) (Fig. 5) is now commonly used, which has been adapted for SR by Momose [11]. Measurement with the interferometer provides phase shifts in a projection image. After tomographic reconstruction, the value of the X-ray refractive index in each cubic voxel can be determined. As the refractive index differs much more than the absorption coefficient among different materials, a phase-contrast image has a higher contrast than an absorption-contrast image.

A grating-based interferometer is available at BL20B2 and BL20XU. It has been used on various soft tissues such as spinal cord [12], eye lens [13], kidney [14] and a fetus [15]. In the circulatory system, an atherosclerotic plaque was imaged successfully [16]. Recently, an aortic wall was studied extensively by phase-contrast CT at SPring-8. With improvements in the fast scanning technique, it is now possible to obtain phase-contrast tomographic images within 30 min, which has greatly facilitated studies on fresh samples. Hoshino *et al.* [17] showed the deformation of an aortic wall with various degrees of stretching (Fig. 6). This type of dynamic tomographic measurement has made it possible to study density changes in the wall with various degrees of stretching.

Phase-contrast tomography is generally useful for obtaining high contrast in images of soft tissues and organs. Figure 7 shows a slice of a whole human fetus heart obtained by phase-contrast tomography. Not only the muscle fibers but also the branching bundle of the conduction system is clearly observed in the

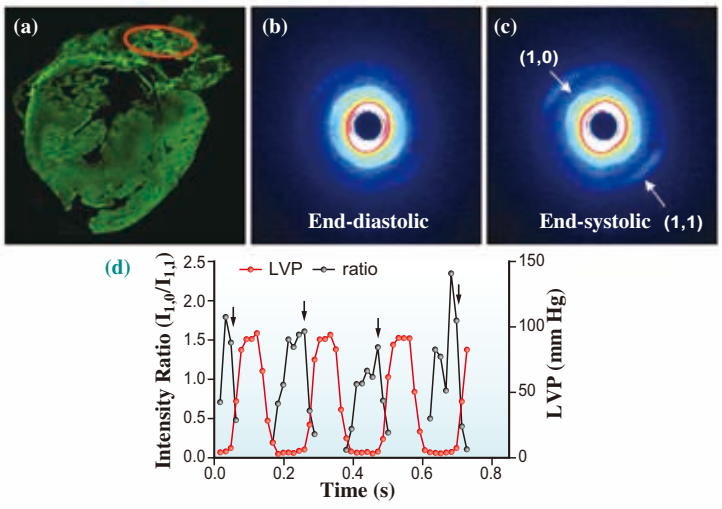

Fig. 4. **(a)** Small-angle X-ray scattering analysis of the red-circled area indicating the iPS cell-derived cardiac myocytes (iPSC-CM) transplanted to an infarcted heart. **(b)** and **(c)** 1,0 and 1,1 equatorial reflections at the end-diastolic and end-systolic phases. **(d)** Myosin mass transfer index (equatorial intensity ratio $I_{1,0}/I_{1,1}$) in an iPSC-CM sheet and simultaneously acquired LV pressure over several consecutive cardiac cycles of an infarcted heart. Significant 1,0 myosin reflections were only evident for part of the cardiac cycle due to heart movement. When significant actin-myosin reflections were evident, the shift in the myosin mass towards actin (decrease in intensity ratio) coincided with the rapid increase in LV pressure during systole, showing synchronized contraction of the iPSC-CMs in the sheet. Arrows indicate the timing of end-diastole.

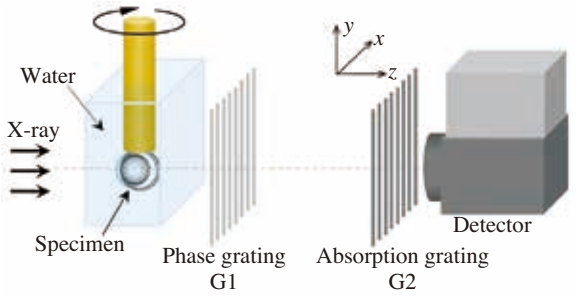

Fig. 5. Schematic diagrams of grating-based interferometer (for Talbot imaging). For each projection image, three to five images are recorded with different shifts of the G2 grating along the x-axis.

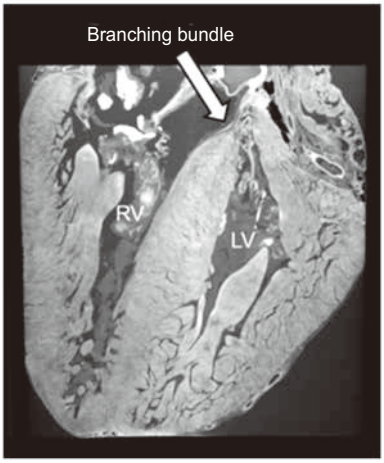

Fig. 7. Cross-sectional image of a whole fetus heart. The branching bundle is clearly observed in the interventricular septum. RV: right ventricle, LV: left ventricle. The formalin-fixed fetus heart was provided by Drs. Yoshihiro Oshima and Makiko Yoshida at Kobe Children's Hospital.

interventricular septum without any excision of the sampMedicalle [18]. As knowledge of conduction system anatomy is critical to prevent complete heart blockage as a complication of repair, the application of phase-contrast tomography may help great progress to be made in evaluating the conduction system anatomy in the case of various congenital heart defects.

Future prospect

Despite the plethora of studies investigating the mechanisms for cardiovascular dysfunctions, the origin of most cardiovascular diseases is still unknown. This high prevalence of idiopathic pathologies has stemmed, at least in part, from the inability to reliably assess the structural and functional properties of the heart and vascular system because of methodological constraints. The development of SR techniques in SPring-8 now holds out the promise of rapid advancement of our understanding of the cardiovascular structure and function. Since cardiovascular research requires a variety of experimental approaches, the combined use of SR techniques, not only those mentioned in this review, will further promote the elucidation of mechanisms and the development of better treatment and prevention of cardiovascular diseases.

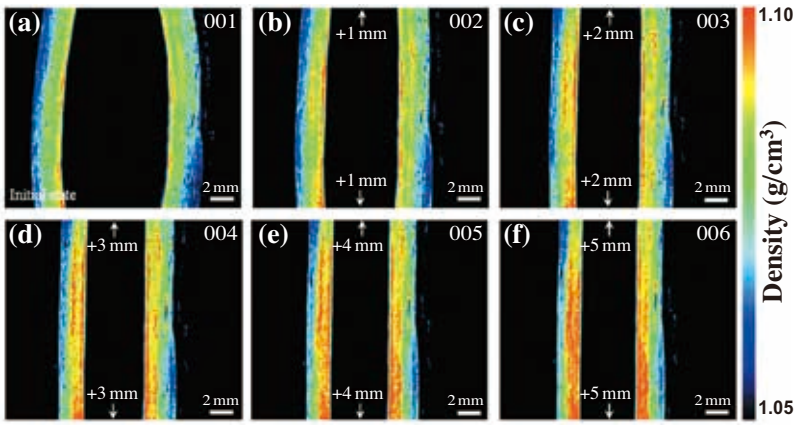

Fig. 6. X-ray phase contrast computed tomography images of a ring-shaped fresh pig aorta subjected of stretching. **(a)** Initial state. **(b)–(f)** Stretched by hooks by multiples of 2 mm (1 mm by the upper hook and 1 mm by the lower hook).

Mikiyasu Shirai[a] and Naoto Yagi[b]

[a] National Cerebral and Cardiovascular Center
[b] SPring-8/JASRI

E-mail: shirai@ri.ncvc.go.jp,
yagi@spring8.or.jp

References

[1] M. Shirai *et al.*: Circ. Res. **112** (2013) 209.
[2] M.J. Jenkins *et al.*: Arterioscler. Thromb. Vasc. Biol. **32** (2012) 370.
[3] D.O. Schwenke *et al.*: J. Appl. Physiol. **110** (2011) 901.
[4] D.O. Schwenke *et al.*: Pflug. Arch. Eur. J. Physiol. **462** (2011) 397.
[5] T. Sonobe *et al.*: J. Appl. Physiol. **111** (2011) 75. (highlighted in Research Frontiers 2012)
[6] I. Matsubara: Ann. Rev. Biophys. Bioeng. **9** (1980) 81.
[7] N. Yagi *et al.*: Biophys. J. **86** (2004) 2286.
[8] J.T. Pearson *et al.*: Circulation **109** (2004) 2983. (highlighted in Research Frontiers 2004)
[9] T. Higuchi *et al.*: Cell Transplant. DOI: 10.3727/096368914X685799 (2015).
[10] U. Bonse and F. Busch: Prog. Biophys. Molec. Biol. **65** (1996) 133.
[11] A. Momose: Opt. Express **11** (2003) 2303.
[12] K. Takashima *et al.*: J. Synchrotron Rad. **22** (2015) 136.
[13] M. Hoshino *et al.*: PLoS ONE **6** (2011) e25140. (highlighted in Research Frontiers 2011)
[14] J. Wu *et al.*: Kidney Int. **75** (2009) 945. (highlighted in Research Frontiers 2009)
[15] M. Hoshino *et al.*: Biol. Open **1** (2012) 269.
[16] M. Shinohara *et al.*: Am. J. Physiol. **294** (2008) H1094. (highlighted in Research Frontiers 2008)
[17] M. Hoshino *et al.*: J. Synchrotron Rad. **21** (2014) 1347.
[18] T. Tsukube *et al.*: Gen. Thorac. Cardiovasc. Surg. (2015) - in press.
Also read Pearson *et al.* in this volume.